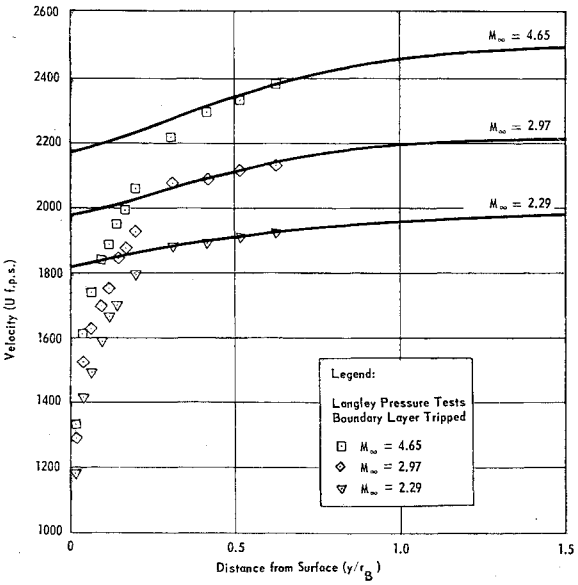

Fig. 2 Shear layer velocity profiles on blunted cylinder $r_B/R_N = 1.667$, $C_{D_N} = 0.25$.

drag coefficient. Because ω_2 appears in the integrand of I_2, an iterative process is required for the calculation. ω_1 is found from Eq. (8) for prescribed values of M_∞, γ, and r_B/R_N. The calculated values of ω_1 and ω_2 together with Eq. (5), then, give the distance from the body surface at which the shear layer properties are obtained.

Experimental data suitable for checking the present method generally are not available, particularly at the higher Mach numbers. For the two-dimensional case Ref. 9 gives velocity and Mach number profiles at a Mach number of 4.7. The data of Ref. 9 for the 0.062-in. leading edge radius are plotted in Fig. 1 for two downstream stations, 0.933 and 1.099 ft. Velocity and Mach number distributions given by the present method with $C_{D_N} = 1.2$ for the cylindrically blunted nose also are shown and compare favorably with the experimental values outside the boundary layer. For the three-dimensional case, velocity profiles obtained at Mach numbers of 2.29, 2.97, and 4.65 shown in Fig. 2 are compared with experimental data obtained from wind-tunnel tests of a non-hemispherically blunted cylinder. The theoretical velocity distributions were obtained for $r_B/R_N = 1.667$ and a nose drag coefficient of 0.25, which is an average value for the range of Mach numbers presented. Again, the experimental points compare well with the theoretical curve outside the boundary layer.

Figure 3 shows typical shear layer Mach number profiles calculated at $M = 20$ for a hemispherically blunted cylinder at constant values of $\gamma = 1.2$, 1.4 ,and 1.67. Since the dynamic pressure is given by the square of the Mach number ratio, it is seen that, beyond about 1.5 body radii, the greatest defect in dynamic pressure occurs for frozen ($\gamma = 1.67$) flow. As far as 8 body radii from the surface, the dynamic pressure is only 39% of freestream for frozen flow but is 93% of freestream for equilibrium ($\gamma = 1.2$) flow. These results are indicative and must be qualified by the actual variation in γ as one moves outward in the flow from the body streamline. Nevertheless, the thermodynamic state of the gas incident upon control surfaces is demonstrably significant.

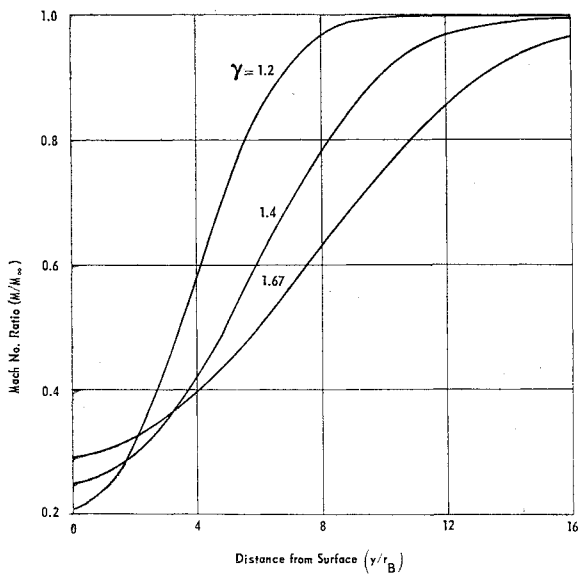

Fig. 3 Shear layer Mach number distribution at $M = 20$ on hemispherically blunted cylinder $C_{D_N} = 0.9$.

References

[1] Moeckel, W. E., "Some effects of bluntness on boundary layer transition and heat transfer at supersonic speeds," NACA Rept. 1312 (1957).

[2] Li, T.-Y., "Simple shear flow past a flat plate in an incompressible fluid of small viscosity," Renesselaer Polytech. Inst., Rept. TR AE 5813 (July 1958).

[3] Murray, J. D., "The boundary layer on a flat plate when the main stream has a uniform shear," Div. Eng. Appl. Phys., Harvard Univ. (June 1958).

[4] Ting, L., "The boundary layer on a flat plate in the presence of a shear flow with large vorticity," Polytech. Inst. Brooklyn Aeronaut. Lab. Rept. 524 (July 1959).

[5] Seiff, A. and Whitney, E., "The effect of the bow shock wave on the stability of blunt-nosed slender bodies," U.S. Air Force, NASA Joint Conference on Lifting Manned Hypervelocity and Re-entry Vehicles, Part I (April 1960).

[6] Hayes, W. D. and Probstein, R. F., *Hypersonic Flow Theory* (Academic Press, Inc., New York, 1959), pp. 204-205.

[7] Traugott, S. C., "An approximate solution of the direct supersonic blunt-body problem for arbitrary axisymmetric shapes," J. Aero/Space Sci. 27, 361–370 (May 1960).

[8] Morkovin, R. V., private communication (August 1961).

[9] Tendeland, T., Nielsen, H. L., and Fohrman, M. J., "The flow field over blunted flat plates and its effect on turbulent boundary-layer growth and heat transfer at a Mach number of 4.7," NASA TN D-689 (February 1961).

Manual Extraterrestrial Guidance and Navigational System

PAUL B. LIEBELT*
The Boeing Company, Seattle, Wash.

IT often is postulated that a fully or semiautomatic guidance and navigational system is required for lunar and solar system missions. If, however, a completely manual system could be devised, it could serve as a back-up system in case of automatic equipment failure, a monitor system for automatic equipment check, or a system to provide initial conditions for automatic equipment after a system shutdown for power conservation or repair.

Presented at the ARS 17th Annual Meeting and Space Flight Exposition, Los Angeles, Calif., November 13–18, 1962. The author is indebted to Robert Goodstein for suggesting the problem and for helpful criticisms.

* Research Engineer, Electronics Technology Department, Aero-Space Division.

System Description

A guidance and navigational system was devised in which the functions of navigation, smoothing, guidance equation solution, and velocity correction could be performed manually using hand-operated devices. The equipment selected includes an angle measuring device with a resolution of 10 arc-sec, a mechanical clock-stop watch combination, a circular slide rule with extended scales to four significant figures, prepared data forms, and prepared star maps.

The method of navigation chosen is essentially a method of celestial triangulation. Two near celestial bodies and a preselected star are sighted and the three included angles $\boldsymbol{\alpha} = (\alpha_1, \alpha_2, \alpha_3)$ between the extremities of the celestial objects are measured. It is assumed tactfully that adequate attitude stabilization exists so that such measurement is possible. These three measurements and the known time-varying distance between the two celestial bodies are sufficient to determine the position of the vehicle. In practice it is not convenient to measure the three angles simultaneously and, in fact, there is no need that this be done. The suggested navigational procedure is to measure the three angles sequentially with a sextant during a prescribed time interval starting at a preselected time. The times at which the measurements occur are noted using the navigational clock. The method of navigation by triangulation was chosen since it blended well with the manual concept, but certainly other schemes would be suitable.

The smoothing technique selected is nonoptimum in the sense of minimum variance and in being unbiased. It is suggested that the measured angular data be plotted and the human eye be used to determine the graphs of the three measured angles as a function of time for relatively short periods of time. The reference values of the measured angles, obtained from a reference trajectory, will be preplotted to aid the eye-fit. This analog technique is suggested for the following reasons:

1) The human as a computer is not capable of finding the optimum estimate of the vehicle's position and velocity based on a series of angular measurements over a long time interval because of the great amount of required computation. Even the simpler analytical formulas for finding the optimum estimate of the graph of the measurements for short periods of time are complex and tedious to apply.

2) For preprogramed time intervals, the measured angles do not change radically as a function of time except at isolated points. Therefore, the scale needed for a graph can be expanded so accuracy in the range of 10 arc-sec in angle and 10 sec of time will be available.

3) Gross measurement and computational errors are eliminated because of the presence of the nominal measured angle values in graphic form. The reference values also serve as a guide to shape the graph of the measured angles.

Figure 1 illustrates the plotting and smoothing phase of the navigator's program. The numbers were obtained from a simulation of a lunar mission. The top chart is the original prepared chart for the angle α_1 on which the measured data are to be plotted and where the nominal value α_{1n} of α_1 is already plotted. The middle chart shows how the angle α_2 was plotted. The third chart illustrates a completed chart. The navigator has drawn his best estimate of the α_3 curve and has interpolated to estimate α_3 at the time of 6 hr. It must be emphasized that the graphs are not to scale and, therefore, do not illustrate the fact that resolution in the 10 sec in arc and in time was achievable.

A computational procedure must be defined now to enable the navigator to transform the interpolated values of the measured angles at two times t_m and t_{m-1} to a time interval and direction of thrust. Using first-order theory, it can be shown that the velocity-to-be-gained $\mathbf{V}_g = (V_{g1}, V_{g2}, V_{g3})$, at a time t_f, has the form

$$\mathbf{V}_g = G_1 \Delta\boldsymbol{\alpha}(t_m) + G_2 \Delta\boldsymbol{\alpha}(t_{m-1})$$

where $\Delta\boldsymbol{\alpha}(t)$ represents the difference of the interpolated angles $\boldsymbol{\alpha}(t)$ and stored value of the corresponding angles on a nominal reference trajectory. The three-dimensional square matrices G_1 and G_2 are precomputed and stored on the navigator's prepared work sheet. The values of the elements of G_1 and G_2 depend upon the mission criteria to be satisfied and upon the guidance philosophy such as minimum fuel, intercept at fixed time, etc.

The time interval of thrust ΔT is computed as, using a nominal value of the acceleration level A,

$$\Delta T = V_g/[A + (A^2 + 2V_gA)^{1/2}]$$

and the direction of thrust (γ, δ) relative to the stars is

$$\gamma = \tan^{-1}(V_{g2}/V_{g1})$$

$$\delta = \tan^{-1}[V_{g3}/(V_{g1}^2 + V_{g2})^{1/2}]$$

For very long missions it will be necessary to correct or reset the navigational clock. This can be accomplished readily by first observing and measuring an additional quantity (e.g., the angular position of a moon of Jupiter). Then, by evaluating an additional linear equation, a correction to the navigational clock can be found.

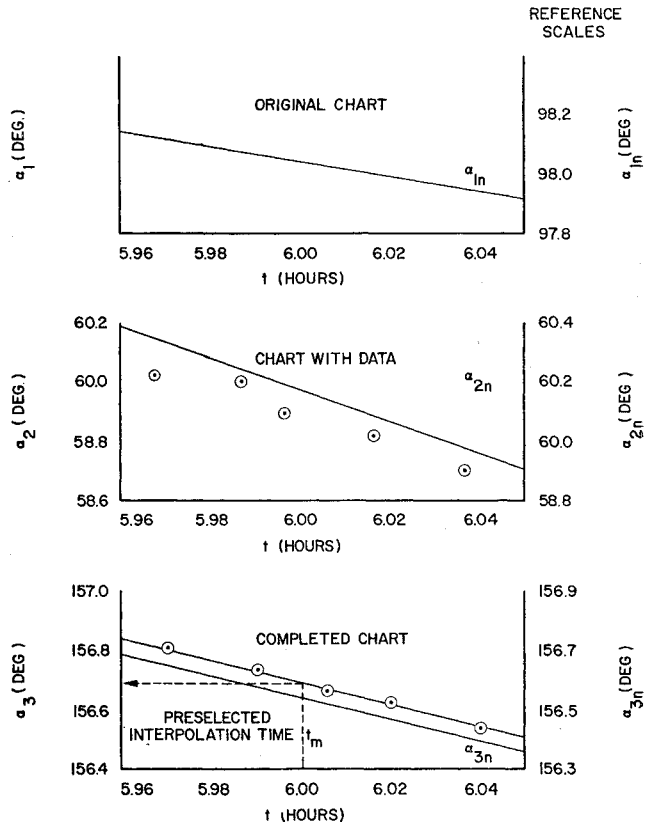

Fig. 1 Measurement, plotting, and smoothing.

The exact procedures used for velocity correction depend upon the vehicle's thrust equipment. In general, however, the astronauts must orient the vehicle and/or the rocket motors so that thrust will occur in the direction (γ, δ) given by the guidance equations. One method of accomplishing this would entail plotting the direction (γ, δ) on a star map transparency, affixing the transparency to optics colinear with the thrust motors, and then manually orienting the vehicle and its equipment so that the transparency image and the actual stars coincide.

After the vehicle or its rocket motors are oriented properly, the thrust maneuver starts at time t_f and is monitored by means of a stop-watch with thrust termination occurring after a time interval of ΔT sec.

System Evaluation

The practicability of the proposed manual system rests upon certain premises. First, the navigator must have the ability to collect a sufficient amount of data during a prescribed interval and to perform the necessary computations within a specified interval without error. Also, the astronauts must be capable of orienting the vehicle relative to a star reference, holding this orientation for the interval of thrust, and terminating thrust within a certain time error. Finally, the approximation of the system must not produce intolerable errors.

A navigator's ability to measure 12 or more time varying angles with an accuracy of 10 sec of arc in a short time interval (about 30 min for a lunar mission) and to orient the vehicle using a star reference can be rested only by simulation. Such experiments were not undertaken.

An estimate of the required time for computation, however, was made. A series of experiments was performed using a simulated lunar mission to measure the interval of time required for equation computation. The navigator's program for two velocity corrections was evaluated a number of times. The average time interval of calculation for one velocity correction was 24 min, which includes the plotting and computation but not the angle measurement interval. The computations were performed with an ordinary slide rule and the results were sufficiently accurate.

A first-order analytical error analysis of the manual guidance and navigation system was undertaken using a typical lunar mission. The components of independent error source vector $\mathbf{E}$ were chosen to be in initial injection position $\mathbf{X}_0$, the measured angles $\boldsymbol{\alpha}$, the time axis of the interpolation graph t, thrust termination timing τ, and thrust orientation $\rho = (\gamma,\delta)$. The errors in these variables were assumed to be Gaussian and uncorrelated with means of zero. The covariance matrix cov($\mathbf{E}$) of these variables is diagonal and the diagonal elements were taken as

$$[\sigma\mathbf{X}_0^2,(\sigma_\alpha^2 + \dot{\alpha}^2\sigma_t^2)/N, A^2\sigma_\tau^2 + 2|\mathbf{V}_g|^2\sigma_\rho^2]$$

where N is an empirical number representing the improvement of the accuracy of the interpolated angles due to the graphical smoothing process. The diagonal elements represent three classes of error: initial position, measurement data reduction, and execution of velocity correction. The dependent variables to be examined for error were the position and velocity $\mathbf{F} = (x,y,z,\dot{x},\dot{y},\dot{z})$ at various times along the trajectory. The covariance matrix cov($\mathbf{F}$) of the final position and velocity was approximated as

$$\text{cov}(\mathbf{F}) \approx (\partial\mathbf{F}/\partial\mathbf{E})^T\text{cov}(\mathbf{E})(\partial\mathbf{F}/\partial\mathbf{E})$$

where the symbol T denotes the transpose and where $(\partial\mathbf{F}/\partial\mathbf{E})$ represents a 6×9 matrix whose elements are the derivatives of the final variables with respect to the independent error source variables. Figure 2 gives typical numerical results of finding the square roots of eigenvalues of cov($\mathbf{F}$) at critical times along the lunar trajectory. The numbers are pessimistic since a conservative upper bound on $\mathbf{V}_g$ was used, no improvement was assumed in using redundant data ($N = 1$), and no attempt was made to minimize the value of the guidance constants by proper choice of stars or times of the measurement taking and course correction.

The equation errors of the manual system were examined for a number of typical lunar trajectories. It was found that if the maximum deviation from the nominal is less than 400 naut miles, the resulting errors due to equation approximation in the neighborhood of the moon were less than 1 naut mile in position and 1 fps in velocity. If, however, large deviations from the nominal are expected, the guidance constants, the elements of G_1 and G_2, can be made as linear or higher order functions of the deviations of $\Delta\alpha$ from nominal to circumvent equation error. This will increase the computation load upon the navigator but not intolerably.

MAXIMUM ERRORS IN EARTH GEOCENTRIC RECTANGULAR COORDINATES

	t	σ_x	σ_y	σ_z	$\sigma_{\dot{x}}$	$\sigma_{\dot{y}}$	$\sigma_{\dot{z}}$
	hr	n.mi.	n.mi.	n.mi.	fps	fps	fps
FIRST CORRECTION	9	3.4	43.1	29.0	11.3	14.7	1.9
SECOND CORRECTION	63	1.6	12.1	7.6	5.1	5.4	3.7
MOON VICINITY	77	54.5	36.8	24.1	14.0	2.4	1.3

PARAMETER ASSUMPTIONS

- SMOOTHING IMPROVEMENT FACTOR N=1
- VELOCITY CORRECTION MAGNITUDE $|V_g|$ = 200 fps.

INPUT ERROR ASSUMPTIONS

- INITIAL POSITION $(\sigma_x, \sigma_y, \sigma_z)$ = (1,1,1) n. mi.
- ANGULAR MEASUREMENT AND PLOT $(\sigma_{\alpha 1}, \sigma_{\alpha 2}, \sigma_{\alpha 3})$ = (10,10,10) sec
- TIME MEASUREMENT AND PLOT σ_t = 10 sec.
- THRUST TIMING σ_τ = .1 sec
- THRUST ORIENTATION σ_ρ = 1 deg

Fig. 2 System error analysis.

Conclusion

A completely manual extraterrestrial guidance and navigation system is feasible from a computational point of view. The ability of an astronaut to obtain sufficient measurement data during a short time interval is yet to be demonstrated. The technique of manually orienting a vehicle to a preferred direction and to perform a velocity correction has been demonstrated by the Mercury flights. The somewhat degraded accuracy of a manual system over an automatic system is to be expected. These considerations indicate that the design and study of a manned system for emergency backup or monitor should be pursued with the utmost vigor.

Body Force Effects on Transient Melting and Vaporizing Ablation

SHIH-YUAN CHEN*
The Boeing Company, Seattle, Wash.

A space vehicle or a ballistic missile re-entering the earth's atmosphere experiences a large aerodynamic drag force in the dense atmospheric region. This drag force, in turn, produces a decelerated motion to slow down the vehicle or missile along its trajectory. In general, ground static transient tests of melting ablation will not be able to simulate this type of decelerated motion. An analysis is made to determine body force effects due to acceleration or deceleration in the stagnation region for melting glassy materials. Within the ranges of values investigated, the results indicate that the transient static tests predict an ablation rate that can be either as much as 23% higher than

Received by ARS December 10, 1962; revision received June 28, 1963. The author wishes to express his gratitude to B. F. Beckelman, Chief of Flight Technology, Aero-Space Division, The Boeing Company, for his interest, encouragement, and permission to publish this material; to H. Kennet, O. A. Huseby, and M. B. Donovan, all of the Advanced Research Section, for their valuable suggestions and comments; and to S. L. Adams for her typing.

* Chief, Advanced Research Section, Flight Technology Department, Aero-Space Division. Associate Fellow Member AIAA.